Size-resolved dynamics of indoor and outdoor fluorescent biological aerosol particles in a bedroom: A one-month case study in Singapore

Running title: Indoor and outdoor bioaerosols dynamics in a bedroom

Jiayu Li [a, †], Man Pun Wan [b], Stefano Schiavon [c], Kwok Wai Tham [d], Sultan Zuraimi [a], Jinwen Xiong [b], Mingliang Fang [e], Elliott Gall [f]

[a] *Berkeley Education Alliance for Research in Singapore, 138602, Singapore*

[b] *School of Mechanical and Aerospace Engineering, Nanyang Technological University, 50 Nanyang Avenue, Singapore 639798, Singapore*

[c] *Center for the Built Environment, UC Berkeley, 390 Wurster Hall, Berkeley, CA, 94720, USA*

[d] *Department of Building, School of Design and Environment, National University of Singapore, 4 Architecture Drive, Singapore 117566, Singapore*

[e] *School of Civil and Environmental Engineering, Nanyang Technological University, 639798, Singapore*

[f] *Mechanical and Materials Engineering, Portland State University, Portland, OR 97201, USA*

[†] The corresponding author: Jiayu Li (ORCID: 0000-0002-5398-1151)

Address: 1 Create Way, #11-02 Create Tower, Singapore 138602

Email: jiayu.li@berkeley.edu

Tel: +65 8525 1223

Acknowledgement

This research was funded by the Republic of Singapore's National Research Foundation through a grant to the Berkeley Education Alliance for Research in Singapore (BEARS) for the Singapore-Berkeley Building Efficiency and Sustainability in the Tropics (SinBerBEST) Program. BEARS has been established by the University of California, Berkeley as a center for intellectual excellence in research and education in Singapore.

Abstract

This study evaluated the interrelations between indoor and outdoor bioaerosols in a bedroom under a living condition. Two wideband integrated bioaerosol sensors were utilized to measure indoor and outdoor particulate matter (PM) and fluorescent biological airborne particles (FBAPs), which were within a size range of 0.5-20 μm. Throughout this one-month case study, the median proportion of FBAPs in PM by number was 19% (5%; the interquartile

range, hereafter) and 17% (3%) for indoors and outdoors, respectively, and those by mass were 78% (12%) and 55% (9%). According to the size-resolved data, FBAPs dominated above 2 and 3.5 μm indoors and outdoors, respectively. Comparing indoor upon outdoor ratios among occupancy and window conditions, the indoor FBAPs larger than 3.16 μm was dominated by indoor sources, while non-FBAPs were mainly from outdoors. The occupant dominated the indoor source of both FBAPs and non-FBAPs. Under awake and asleep, count- and mass-based mean emission rates were 45.9 and 18.7 × 10^6 #/h and 5.02 and 2.83 mg/h, respectively. Based on indoor activities and local outdoor air quality in Singapore, this study recommended opening the window when awake and closing it during sleep to lower indoor bioaerosol exposure.

Keywords: bioaerosols; WIBS; I/O ratio; indoor air quality; sources of aerosols; residential building

PRACTICAL IMPLICATIONS:

- Developing knowledge about the indoor and outdoor relationship of PM and bioaerosols in a bedroom under a living condition in Singapore can help us better understand the human exposure levels in this scenario.
- The findings from this study help in understanding of sources of different particles in a bedroom. Human or human-related activities were the major indoor source of bioaerosols, while non-biological particles are more from outdoors. This study adds quantitative information about human emissions in a bedroom during awake and sleep periods, respectively, which can be used in the indoor air quality model and design of mitigating strategies.
- From this study, opening or closing the window is a simple and effective way to lower indoor bioaerosol exposure. Whether we should keep the window open or closed can base on the station outdoor PM level and indoor activities, which can suggest people on window opening behaviors and to design "smart" windows to open or close automatically.

1. INTRODUCTION

Exposure to airborne particulate matter (PM) can have a significant impact on human health[1–4]. Their health impacts are usually linked with the type and size of particles and exposure levels[5,6]. As a subset of PM, biological aerosol particles, or bioaerosols, constitute a significant proportion of PM in both indoor and outdoor environments[7–9]. Exposures to bioaerosols could have a higher health risk than exposures to non-biological particles, in terms of, infectious diseases, allergies, and cancer[10,11]. Singapore is a humid island tropical country with one of the highest population densities, and the local meteorological condition

and ecological environment generally favour the proliferation of flora and fauna, which could have a higher potential of bioaerosol exposure risk[12–15].

People spend more than a third of their life in their bedroom[16–18]. The air quality of bedrooms affects peoples' sleep quality[19], health[17,20], and next-day productivity[21]. In Singapore, 81% of residents live in public housing[22], locally referred to as the Housing & Development Board (HDB) building, which are normally naturally ventilated and are without air filtration systems. Therefore, opening the window(s) could be the only, or main method of, diluting the indoor generated pollutants by naturally ventilating the space. However, a higher ventilation or air exchange rate could allow more outdoor particles infiltrate indoors. Hence, to create a healthier bedroom environment, we need to have a better understanding of the levels and relationship of indoor and outdoor PM and bioaerosols.

In the past, the most widely used methods to study bioaerosols were culture-based[23]. However, only culturable microorganisms, a subset of the viable bioaerosols, can be measured with this approach. Though non-viable bioaerosols cannot cause infectious diseases, they still can cause allergic and toxic reactions[24]. Since less than 1% of bioaerosols are culturable[25], techniques beyond culturing are required to understand the entirety of both indoor and outdoor bioaerosols. Molecular methods, such as DNA- or RNA-based sequencing techniques, can obtain abundant biological information, but require time and relatively high resource investments. Because both culture-based and molecular techniques are usually off-line analyses, a relatively long duration of incubating, staining, and sequencing after collection of bioaerosols is often needed.

In contrast, light-induced fluorescence (LIF) combined with the optical particle sizer can detect biological particles – via distinctive fluorescence effects of biological molecules[26] – and their respective particle sizes almost instantaneously. Although there is a lack of detailed biological information of the species, these real-time detection techniques are still attractive for long-term campaigns of bioaerosol measurement. Typical instruments include the wideband integrated bioaerosol sensor (WIBS) and the ultraviolet aerodynamic particle sizer (UV-APS)[27]. Moreover, in the process of discriminating particles according to their fluorescent effect, these instruments record information of both biological and non-biological ones simultaneously, which can be used to calculate the proportion of bioaerosol in PM. As the PM concentration is a basic air quality index in many standards and is widely monitored and frequently reported worldwide by stations, if obtained bioaerosol proportions are relatively stable in each condition, these proportions can be used to estimate the bioaerosol exposure according to the easily obtained PM level.

In this study, two units of WIBS were utilized to simultaneously monitor both indoor and outdoor bioaerosols in a naturally ventilated bedroom in Singapore. Because local meteorological parameters and the day length are relatively stable across seasons, a one month was selected as the duration for this experiment. In this case study, with considering

the effect of the occupant and the window on indoor and outdoor bioaerosol dynamics, we sought to answer three questions:

a) What are the indoor and outdoor bioaerosol and PM concentrations and their size distributions for this typical residential case in Singapore?
b) What are the proportions of bioaerosol in the PM for different particle sizes?
c) What is the size-resolved relationship between indoor and outdoor bioaerosols?

2. METHODS

2.1. The bedroom and facilities

For this case study, a naturally ventilated bedroom on the 6th floor of a 12-story HDB building was selected as a case study for monitoring bioaerosols. Inside the bedroom, as shown in Figure 1, there were a king-size bed, a table, a wardrobe, a wall-mounted fan, and an indoor unit of the household air-conditioner (AC). There was no visible mold in the bedroom and the ensuite bathroom.

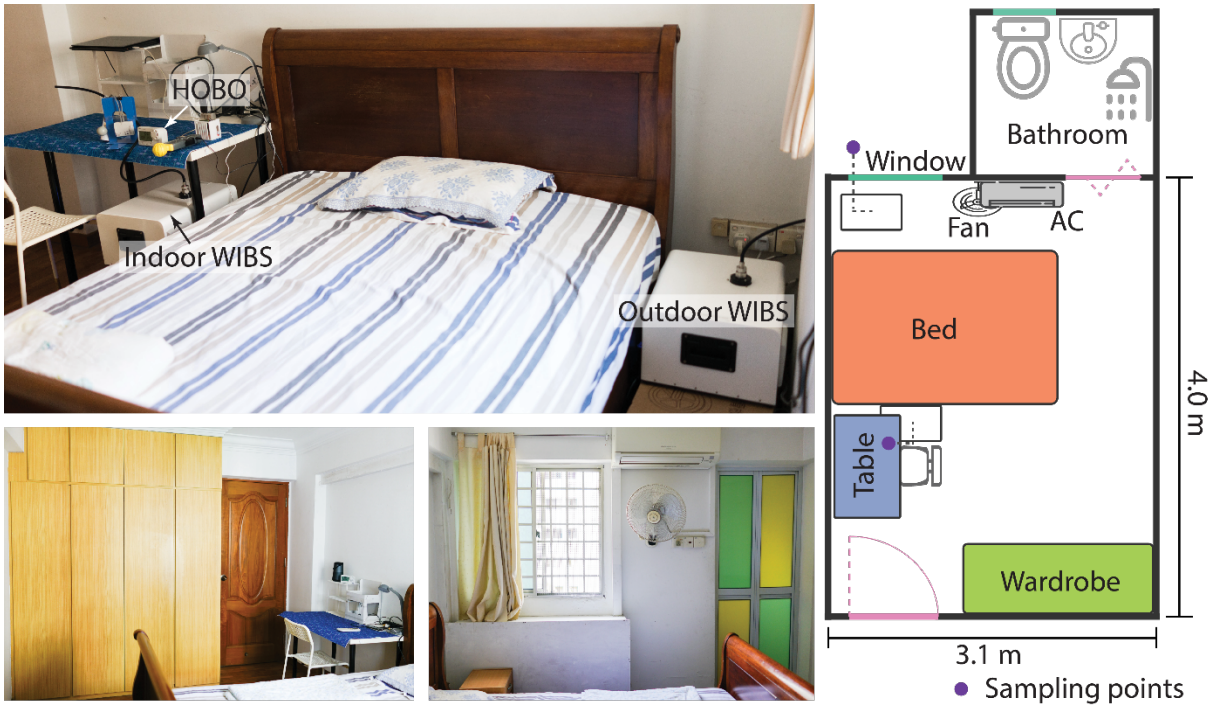

Figure 1. Photograph of the case-study bedroom and its layout

The main instruments utilized in this study were two identical units of the latest version of WIBS (WIBS-NEO, Droplet Measurement Technologies, USA) for indoor and outdoor sampling. The indoor sampling point was set at a breathing zone near the table, where the occupant spent most of the time sitting. The outdoor sampling point was located 50 cm from

the external wall, which was reached using a one-meter conductive silicon tube via a hole on the wall. To collect sufficient data, indoor and outdoor bioaerosol samples were measured for one month from March 23rd to April 20th, 2019. During this period, one male researcher resided in the bedroom to simulate normal living conditions and bedroom activities, such as; sleeping, using a laptop (during most of the time when he was awake), arranging the bedsheets (twice a day), changing and folding clothes (twice a day), and vacuum cleaning (twice a week).

Occupancy and indoor activities were self-recorded. The window conditions were monitored by a smart window/door sensor (MCCGQ01LM, Xiaomi, China), and the usage of the fan and AC were monitored by smart plugs (Mi Smart Plug Wi-Fi, Xiaomi, China). Indoor and outdoor air temperatures and relative humidity (RH) were measured via two temperature and RH sensors (U12-013, HOBO®, the United States). There were two doors, one connected to the living room, and the other to the bathroom. To minimize air exchange between the rooms, new door seals (RP48, RAVEN®, Raven Products Pty. Ltd., Australia) were added for both doors before the start of the experiment. Unless the occupant entered the bedroom or bathroom, the two doors were closed.

2.2. WIBS and particle classification

WIBS features a size-resolved single-particle instrument, which detects each particle in four channels: i.e. one continuous laser channel, and three fluorescent channels. The laser channel functions as an optical particle sizer, which counts the sampled particle and measures its size within the range of 0.5-20 μm. For detecting fluorescent signals of each particle, there are two ultraviolet (UV) Xenon lamps providing the excitations at 280 and 370 nm, and two emission detectors which measure the emissions from 310-400 and 420-650 nm. With the two UV lamps and two detectors, three fluorescent detection channels were defined as: FL1, excited by 280 nm UV and detected at the range 310-400 nm, whereby the biological signature of tryptophan is targeted; FL2 measures the particle excited by 280 nm UV and detected at the range 420-650 nm, but its biological target is still unclear; and FL3, emissions at 420-650 nm after 370 nm excitation are used to detect the presence of nicotinamide adenine dinucleotide phosphate (NADPH)[26].

Although all sampled particles are detected by the laser channel, it should be noted that not all of them can be measured by the fluorescent channels. WIBS uses a diaphragm pump to provide a constant sample flow rate at 5 cm^3/s with a fluctuation less than ± 0.1 cm^3/s. The Xenon flashlamps have a maximum duty cycle of 125 Hz, which can excite and examine, at most, 125 particles/s. When the concentration is higher than 25 particles/cm^3 and the sample air flow rate is 5 cm^3/s, the UV lamps will inevitably miss particles. The missed particles have size information from the laser channel but don't have any signal from fluorescent channels. The examined particles in fluorescent channels are noted as "Excited" particels, and the undetected ones are considered as "Unknown". Excited particles can be further classified as fluorescent and non-fluorescent particles according to their fluorescent strength. Unknown

particles without fluorescent information cannot be classified directly but can be prorated into different types when calculating the concentrations later.

The criteria to examine the Excited particles for fluorescent or non-fluorescent particles is based on the fluorescent background in each fluorescent channels. To get the fluorescence background in each fluorescent channels, one minute's force trigger (FT) tests were performed once per day for both indoor and outdoor units. For each fluorescent channel, the threshold for classifying an Excited particle into a fluorescent particle is that, the measured fluorescence of this particle in the channel is larger than the mean fluorescence of the FT test plus three times its standard deviation (SD, σ)[28], as shown in Eq. (1).

$$fluorescence_{chnl} > fluorescence_{chnl}^{FT} + 3\sigma \quad chnl \in \{\text{FL1, FL2, FL3}\} \tag{1}$$

For excited particles that are not missed by the Xenon flashlamps, each will have three fluorescent intensities in three channels, i.e. FL1, FL2, and FL3. If any of the three fluorescent signals exceed their thresholds, it will be considered as a fluorescent biological airborne particle (FBAP). For all FBAPs, we further classified them into seven subdivision of fluorescent types can be performed according to the three measured channels[29]: A, B & C are the particles that had only reached the threshold of one channel (FL1, FL2 & FL3, respectively) but didn't reach the thresholds of the other two channels; AB, AC & BC are the particles recognized only in two of the three channels; and particles with the type ABC are those that can be detected in all the three fluorescent channels. In contrast, only if the excited particle cannot reach any of the three thresholds, it will be considered as a non-fluorescent particle, noted as non-FBAP. To show the relationship among the detection channels and the related particle type more clearly, the indoor and outdoor particles measured during the month are summarized in Figure 2. Followed by Perring et al.[29], this classification method provides important potential to distinguish species[30]. However, there is still a lack of sufficient evidence for mapping FBAP subtypes to species in field studies (details are discussed in Appendix 1 (S1)).

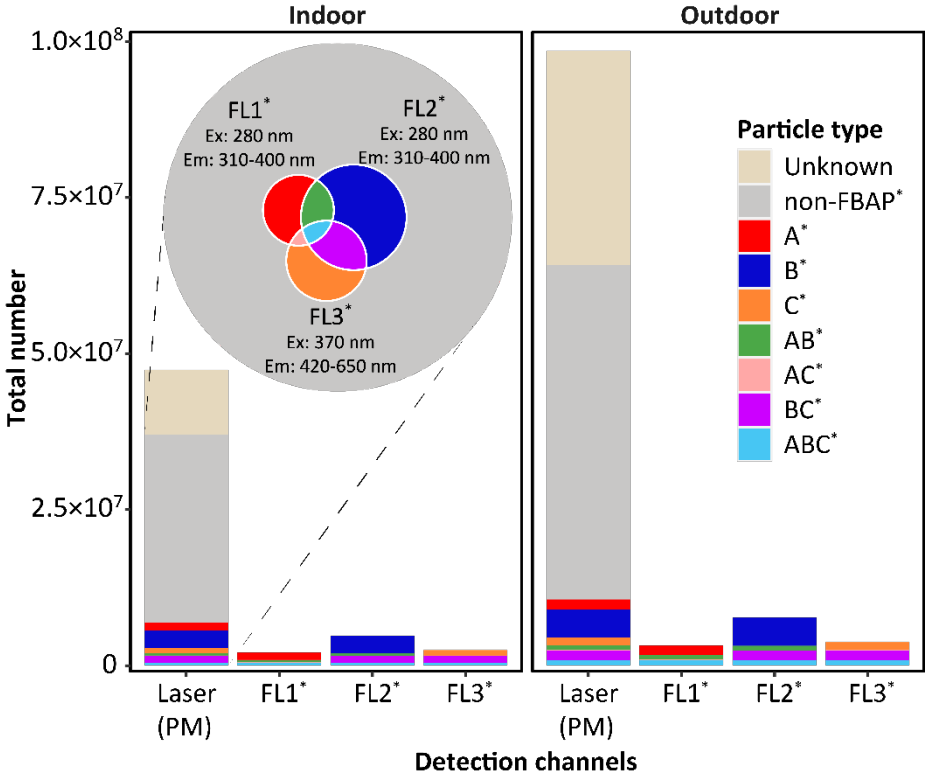

Figure 2. Summary of measured particles in one month (23 Mar – 20 Apr, 2019). Each bar shows the total number of detected particles in the channel, and the color fill of the bar shows the related particle types. The color scheme for different particle types followed a previous study[31]. For indoor particles, the Venn plot was derived from the total number of particles in each channel as a full circle area and each subdivided type as a filled area with different colors.

The relationship among different categorized particle types can be summarized by the Eq. (2). The asterisks in Eq. (2) indicate that the corresponding types of particles have not considered their amount in Unknown particles yet.

$$
\begin{aligned}
&A^* + AB^* + AC^* + ABC^* = FL1^* \\
&B^* + AB^* + BC^* + ABC^* = FL2^* \\
&C^* + AC^* + BC^* + ABC^* = FL3^* \\
&A^* + B^* + C^* + AB^* + AC^* + BC^* + ABC^* = FL1^* \cap FL2^* \cap FL3^* = FBAP^* \\
&FL1^* \cap FL2^* \cap FL3^* = ABC^* \\
&FBAP^* + non\text{-}FBAP^* = Excited \\
&Excited + Unknown = PM
\end{aligned}
\tag{2}
$$

In this study, according to the measured particle diameters (D_p), we classified the particles into 16 size bins from 0.5 to 20 μm with same logarithmic distance ($\mathrm{d}\log D_p$) of 0.1 μm. For PM, Excited and Unknown type of particles, the particle counts in the i^{th} size bin was denoted as N_i^{type}. For other particle types, the real amount of particles need to include the amount of unclassified Unknown type. For each size bin, we assumed that the proportions of these type of particles in Excited and Unknown are the same. Hence, to calculate the real particle amount of each type, we can multiply the amount of PM by the proportion of the classified amount ($N_i^{*,type}$) of this type in Excited, as shown in Eq. (3). Further, the size-resolved number concentration ($C_{N,i}^{type}$, #/cm^3) can be calculated directly by using the measured particle counts at i^{th} size bin (N_i^{type}) divided by the sample flow rate (Q, cm^3/s) and the sampling period (T, s), as shown in Eq. (4). Using an assumed density of 1.67 g/cm^3 for all the particles[32,33], the mass concentration ($C_{M,i}^{type}$, μg/m^3) was calculated in Eq. (5).

$$N_i^{type} = \begin{cases} N_i^{type} & type \in \{PM,\ Excited,\ Unknown\} \\ \dfrac{N_i^{*,type}}{N_i^{Excited}} \cdot N_i^{PM} & type \notin \{PM,\ Excited,\ Unknown\} \end{cases} \quad (3)$$

$$C_{N,i}^{type} = \frac{N_i^{type}}{Q \cdot T} \quad (4)$$

$$C_{M,i}^{type} = \frac{1.67 \times 10^{-6} \cdot \pi \cdot \left(D_p\right)^3 \cdot C_{N,i}^{type}}{6 \cdot Q \cdot T} \quad (5)$$

The data analysis was performed in R programing language using RStudio v1.2.5001. For the R packages used in this study, we used rhdf5 v2.28.1[34], Tidyverse v1.21[35], and data.table v1.12.4[36] to handle the measured raw data in .h5 format. We used ggplot2 v3.2.1[37] for data visualization, and patchwork v0.01[38] to combine plots. The codes and data will be available at https://github.com/JiayuLIAQ/FBAP_bedroom.

2.3. Quality control and uncertainty analysis

To ensure the same performance, both units were sent back to the manufacturer (Droplet Measurement Technologies, USA) for factory calibration just before the experiment. Auto fluorescent monodisperse polystyrene latex (PSL) microspheres (Fluoro-Max, Thermo Fisher Scientific, USA) were used to calibrate the size and fluorescence of particles. As the calibration curve was based on PSL sphere, the reported sizes were an estimation when the particle is not spherical. When the units had returned from their calibration, we double-

checked the performance via a side-by-side comparison test, whereby the two units ran with two calibrated optical particle sizers (OPS) (3330, TSI, USA). The differences between the measured number concentrations from these four instruments for each size bins were less than 10%. To further eliminate the influence of equipment on the indoor and outdoor relationships, two units were alternatively measuring indoor and outdoor, which alternated after seven days.

3. RESULTS

During the one-month experiment, conditions were summarized in Figure 3. The boxplot shows the daily occupied duration and daily usages of the AC, fan and the window.

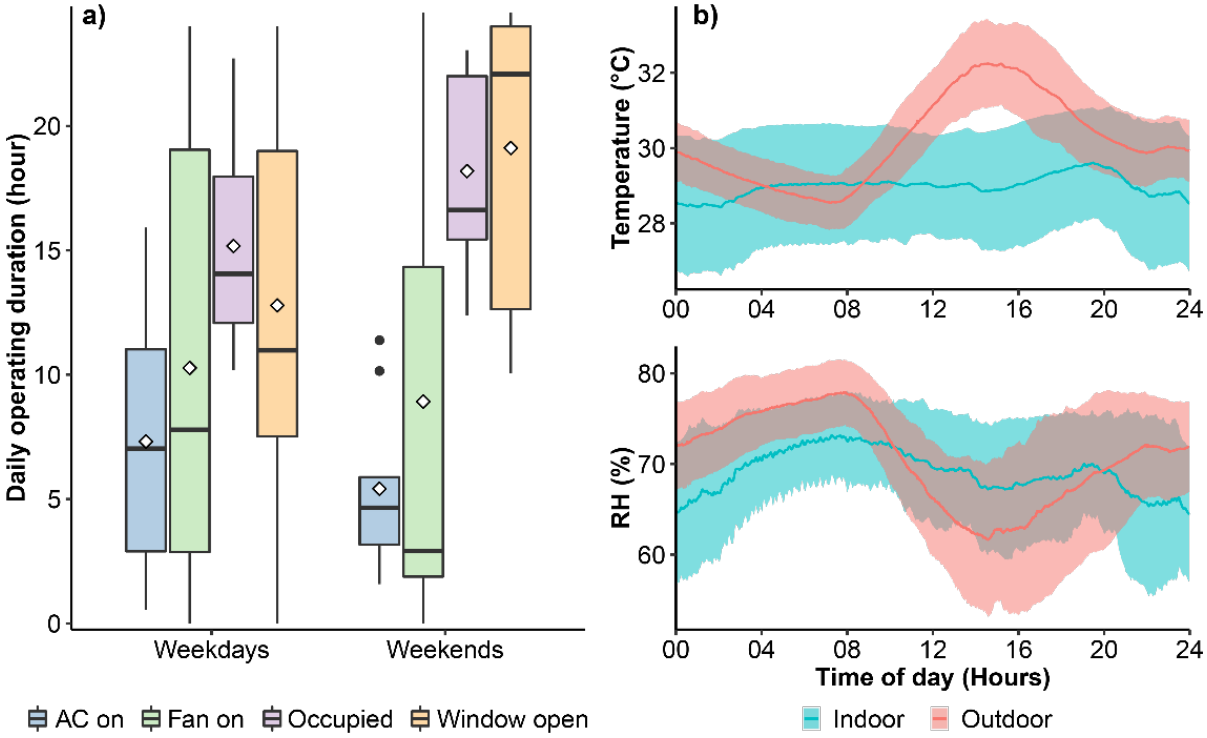

Figure 3. Experimental conditions during the one-month experiments. The filled areas of the boxes are the interquartile ranges (IQR) for daily usage durations. The line in the box is the median, and rhombus dots the arithmetic mean. Whiskers of the boxes start from the upper and lower limits of the box and end at the length of 1.5 times the IQR or at the maximum and minimum values – whichever is reached first. If whiskers end at 1.5 times the IQR, the round dots are the outliers. The ribbon plot shows the variation in the indoor and outdoor temperatures and RH. The lines are the mean values at that time of the day during the one-month experiment and the lower and upper limits of ribbons are mean values minus or plus standard deviations (SD), respectively.

From Figure 3 (a), the occupant spent around 14.7 hours per day in the room during weekdays and about 18.6 hours during weekends. The occupant used the fan more often than

AC, and he tended to keep the window open to have more natural ventilation, especially during weekends when he spent more time at home. During the experiment period, 28% of the time the AC was on, 41% the fan was on, and 61% the window was open. The occupancy and the usage of the AC, the fan, and the window didn't show a clear diurnal pattern (detailed in Appendix 1 (Figure A1)). During the one-month experiment, the window was kept either fully open or closed, the setpoint of the AC was 27 °C when it was on, and the fan was operating at the "middle" level under oscillation mode, which generated the averaged room airflow around 0.2 m/s. As shown in Figure 3 (b), the indoor temperature was between 27 °C and 30 °C for most of the time, which had a higher variation among days than outdoor one according to the width of the ribbons. However, there was less variation for the mean values along the time than outdoor ones, and indoor temperature was lower for most of the time. The indoor RH was around 60% to 75%. Indoor RH was higher than the outdoor one during the daytime, while outdoor RH was higher during nighttime.

3.1. Concentrations and size distributions of indoor and outdoor particles

With the measured one-month particle data, the number concentrations for each day were calculated in different particle types and size bins and plotted in Figure 4.

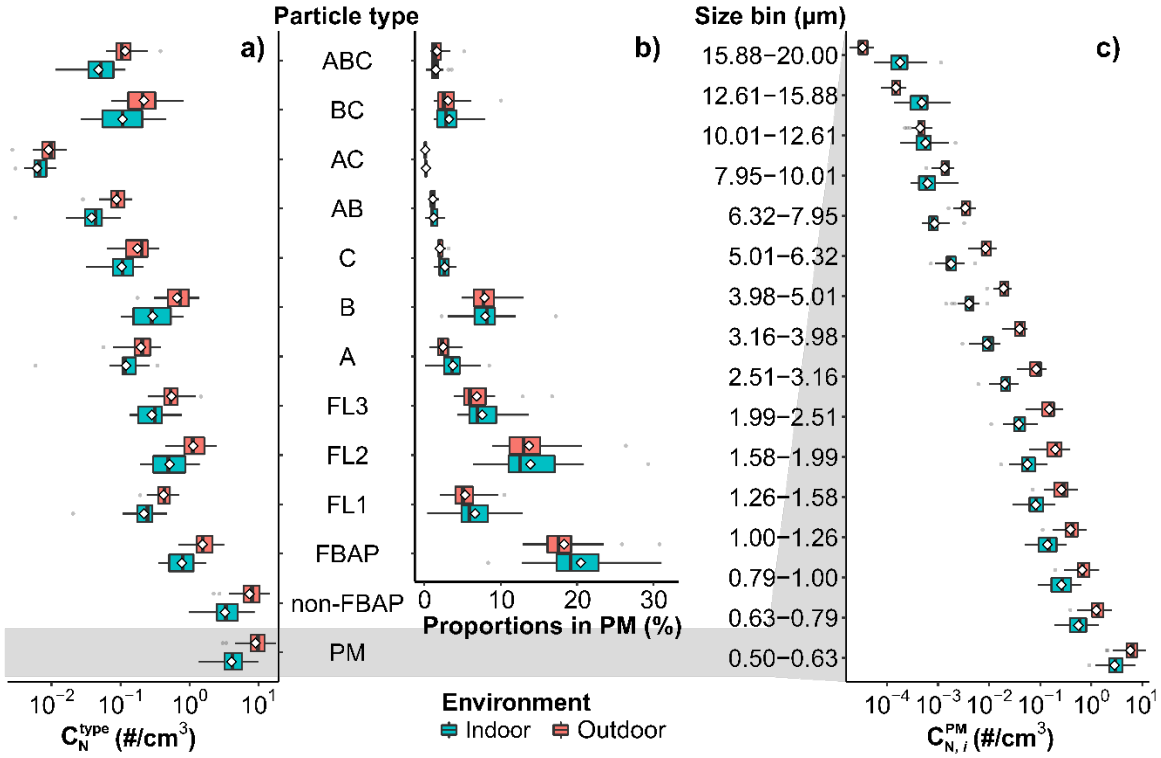

Figure 4. Indoor and outdoor aerosol number concentrations in different type (a). size bins (c), and the fractions of different fluorescent particles in the PM (b). The boxes colored in turquoise are the interquartile range (IQR) for indoor particles, and those colored in red are

the outdoor particles. The statistical symbols have the same meaning as those in Figure 3, thus not repeated here. Statistical data can be found in Table A1–A3 in the Appendix 1.

Figure 4 (a) shows particle number concentrations (#/cm^3) of different types of particle. For all the particle types, both the mean and median number of outdoor concentrations are always higher than those indoors. During the month, the median (IQR) concentrations of PM within the measuring range of 0.5 – 20 μm were 3.7 (2.7) and 7.8 (3.1) #/cm^3 for the indoor and outdoor environments, respectively. Among the total amount of airborne particles, most of them were non-fluorescent. The FBAP have concentrations of 0.7 (0.5) and 1.4 (0.7) #/cm^3 for the indoor and outdoor environments, which contributed 19% (5%) and 17% (3%) of PM by median (IQR), respectively, as shown in Figure 4 (b). By the mass concentration, 78% (12%) and 55% (9%) of PM were indoor and outdoor FBAP, respectively, which were much higher than those by the number concentration. The different size distribution of different particle types will be discussed in the next section. Further, Figure 4 (b) also shows that, for particle types not related with FL2 (FL1, FL3, A, C, AC), indoors always has a higher proportion in PM than outdoors, but for FL2 related types (FL2, B, AB, BC, and ABC), their contribution to PM in indoors and outdoors are similar. If we separate the PM concentrations into different size bins for both indoors and outdoors, we can see from Figure 4 (c) that the number concentration was dominated by the first bins (0.50 - 0.63 μm) with the median (IQR) of 2.4 (1.8) and 4.6 (1.8) #/cm^3, respectively. As the particle size increases, both indoor and outdoor number concentrations decreased exponentially. However, the indoor and outdoor mass concentrations were dominated by 12.51-15.88 μm and 2.51-3.16 μm, respectively (detailed in Appendix 1 (Figure A2)). For the particles with a diameter smaller than 10 μm, outdoors has more particles; however, for the coarser particles larger than 10 μm, the concentration indoors becomes higher.

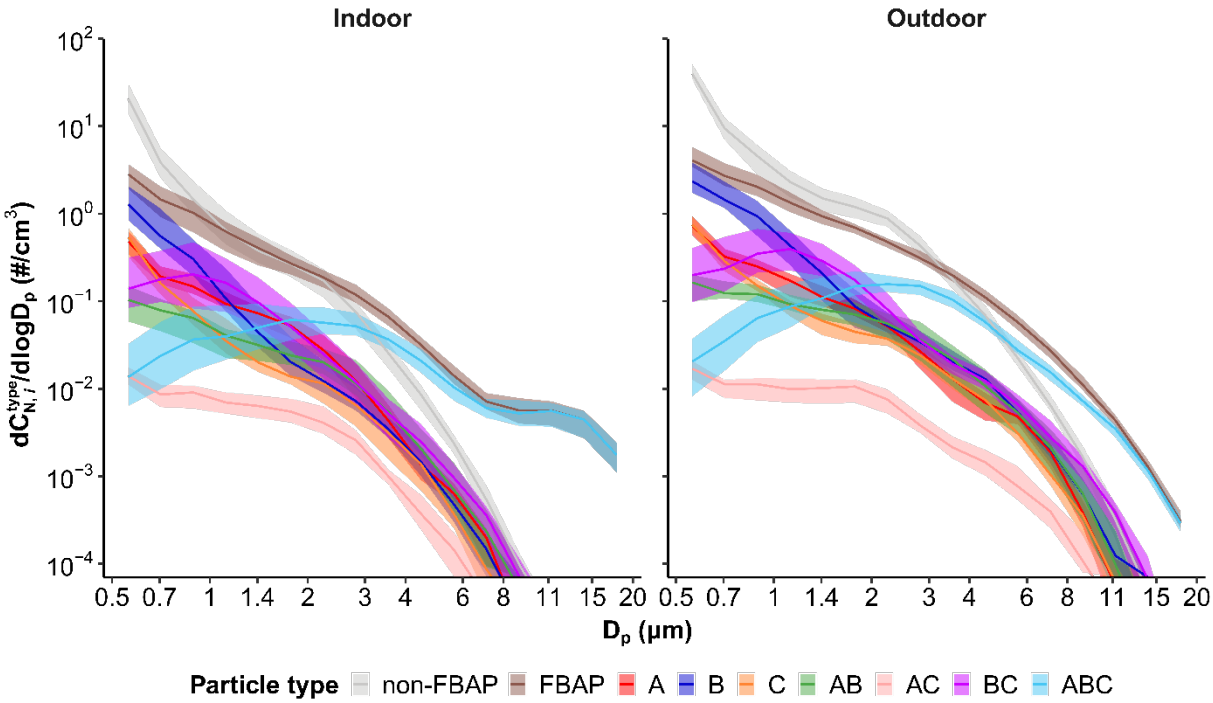

Figure 5. Normalized size distribution for different types of particles. The ribbons are the IQR of the normalized particle concentrations for each particle type, and the solid lines show their median values. Note that the data points for ribbons and lines were middle points (D_p) with the same logarithmic distance between upper and lower levels of size bins. The related data can be found in Appendix 2 (.csv format).

In Figure 5, the particle number concentration is normalized by the logarithmic distance of each size bin. It shows that, for most of the particle types in both the indoor and outdoor environments, concentrations decayed monotonically with increase in particle size. However, for BC and ABC types of fluorescent particles in both indoor and outdoor environments, the highest concentrations were observed between the size ranges of 0.7 – 1 μm and 2 – 3 μm, respectively. If we focused on the total number of FBAP and non-FBAP particles shown in the gray and brown plots in Figure 5, more of smaller particles are non-FBAP and more of the larger ones are FBAP. Indoors FBAPs dominated above 2 μm, and outdoors ones dominated above 3.5 μm. The concentrations of type AC particles were always the lowest for all the sizes. For indoor and outdoor environments, the proportional size distribution of different particles according to the number and mass concentrations were plotted in Figure A3 (Appendix 1), respectively, and the related data can be found in Appendix 3 (.xlsx format)

3.2. Proportions of FBAP in PM

For each size bin in Table 1, proportions of different type of particle in PM were calculated for the indoor and outdoor environments, respectively. It shows that most of the particles in the first size bin (0.50-0.63 μm) are non-FBAPs, and FBAPs only contribute 12%

and 10% of the indoor and outdoor PM, respectively. When particle size increased, the proportions of FBAPs increased. Especially, when FBAPs are smaller than 1 μm, their proportions in each size bin increased dramatically with their size. The proportions of non-FBAP in the indoor environment were always higher than those in the outdoor environment for all size bins, especially for particles within the size range of 1.58 – 10.01 μm. The FBAP proportions indoors could be 10 – 17% higher in the median difference. Other statistical data showing the indoor and outdoor differences of FBAP and other particle types were plotted in a boxplot in Appendix 1 (Figure A4).

Table 1. Proportions of FBAP in PM for each size bin in the indoor and outdoor environments.

Size bin (μm)	Indoor			Outdoor			Δ
	Median	5th	95th	Median	5th	95th	Median
0.50-0.63	12%	7%	20%	10%	7%	16%	2%
0.63-0.79	27%	19%	39%	22%	15%	36%	5%
0.79-1.00	40%	30%	50%	30%	23%	49%	9%
1.00-1.26	46%	38%	59%	38%	27%	59%	8%
1.26-1.58	48%	42%	61%	38%	28%	55%	9%
1.58-1.99	49%	37%	69%	36%	27%	52%	13%
1.99-2.51	50%	36%	72%	35%	25%	51%	15%
2.51-3.16	62%	46%	77%	44%	30%	57%	17%
3.16-3.98	72%	58%	81%	55%	40%	68%	16%
3.98-5.01	79%	68%	89%	64%	49%	75%	15%
5.01-6.32	86%	76%	94%	73%	62%	82%	14%
6.32-7.95	93%	88%	97%	81%	73%	88%	12%
7.95-10.01	98%	95%	100%	87%	79%	93%	11%
10.01-12.61	100%	99%	100%	93%	87%	97%	7%
12.61-15.88	100%	98%	100%	97%	92%	100%	3%
15.88-20.00	100%	100%	100%	100%	93%	100%	0%

The proportions of non-FBAPs and the subdivisions of FBAPs in PM were plotted in Figure 6, and the proportion differences of those particle types between the indoor and outdoor environments were plotted in Figure A4 in Appendix 1. It shows that non-FBAPs contributed less to PM than FBAP when their sizes were larger. The proportions of type ABC increased monotonically along with particle size. When the particle diameter is larger than 2

μm, ABC particles contributed to most of the FBAPs. Especially in the indoor environment, almost all the fluorescent particles were type ABC with the median proportion larger than 98% for particles larger than 10 μm. In both indoor and outdoor environments, type B had the highest proportions in the first three size bins. In the indoor environment, type A had a unimodal distribution with the peak around 1.00-1.26 μm, whilst the proportions of this type in the outdoor environment were bimodally distributed. The first modal of the type A particles in outdoor environment was approximately the same as the indoor peak, and the second modal was larger in size (5.01-6.32 μm). According to a previous study[39] about the interpretation of type A particles, bacteria contributed the first modal, and fungi contributed the second. Thus, we can deduce the proportion of bacteria in PM could be higher in the bedroom than outdoor, while that of fungi could be higher outdoors. For types B and BC, the proportion of outdoor particles were bimodally distributed based on the size with the higher peaks appearing in the larger size bins, whilst those found the indoor environment only show one prominent peak in the smaller size ranges, which aligned with the lower peak of the outdoor environment. For type C and AC, the proportions were relatively small with relatively even distribution along with the size.

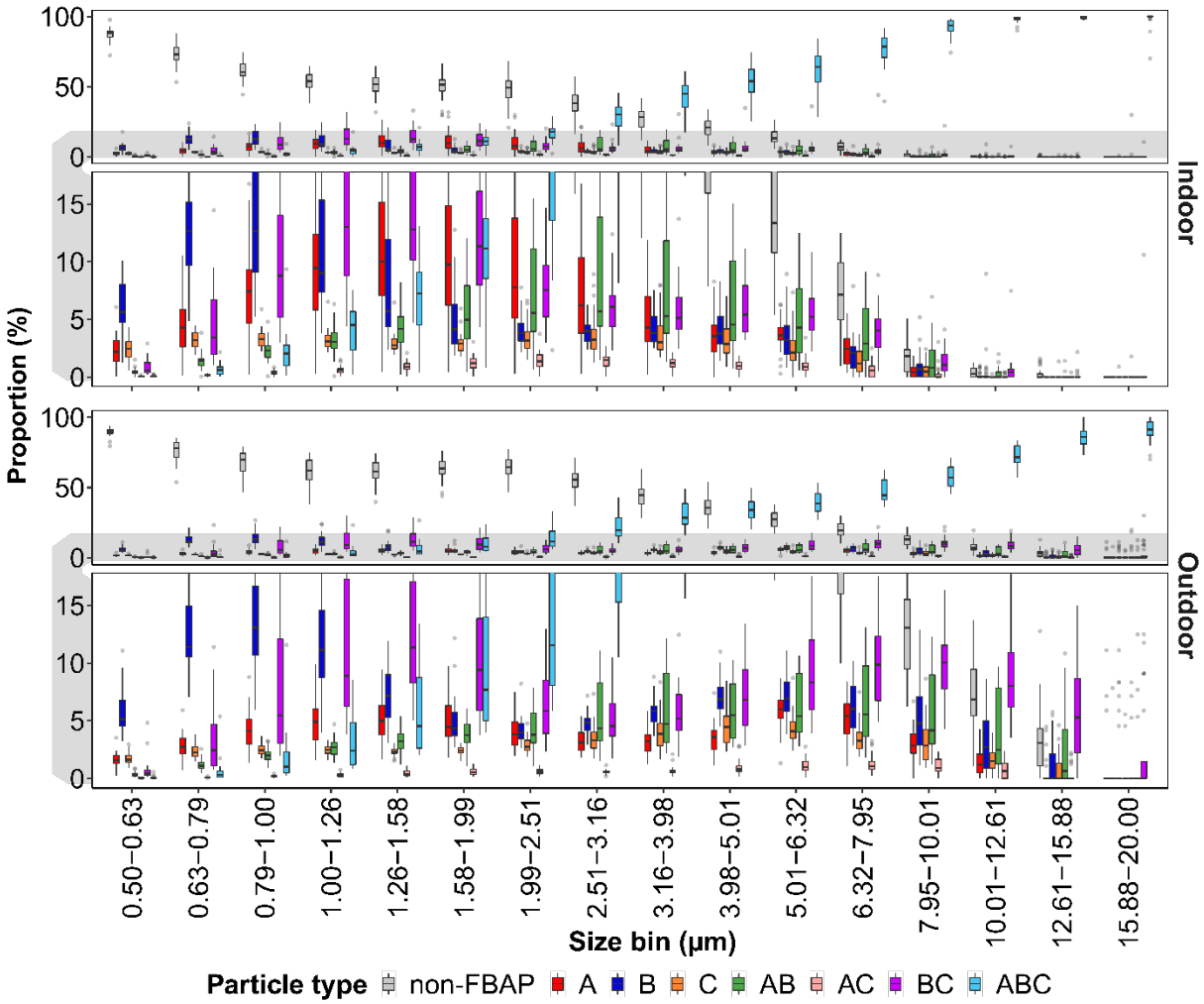

Figure 6. Size-resolved proportions of non-FBAP and subtypes of FBAP in PM in the indoor and outdoor environments. Because there were always one or two types of particle which have much higher proportions than others for both indoor and outdoor environments, the lower parts of the plots have been enlarged (shown as the shaded region) to show them clearly. The related data can be found in Appendix 4 (.xlsx format).

The status of window and occupancy could also affect the difference of PM compositions between the indoor and outdoor environments (detailed in Figure A5 in Appendix 1. Comparing to the overall indoor and outdoor differences listed in Table 1, the differences were larger when the room was occupied and the window was closed. However, when the window was open, the difference of the PM composition was narrowed down because of a higher air exchange rate.

3.3. Effect of window on indoor and outdoor particle dynamics

According to the status of window (i.e. open & closed) and occupancy (i.e. occupied & unoccupied), we further subset the results of the I/O ratio into four parts and plotted this information in Figure 7.

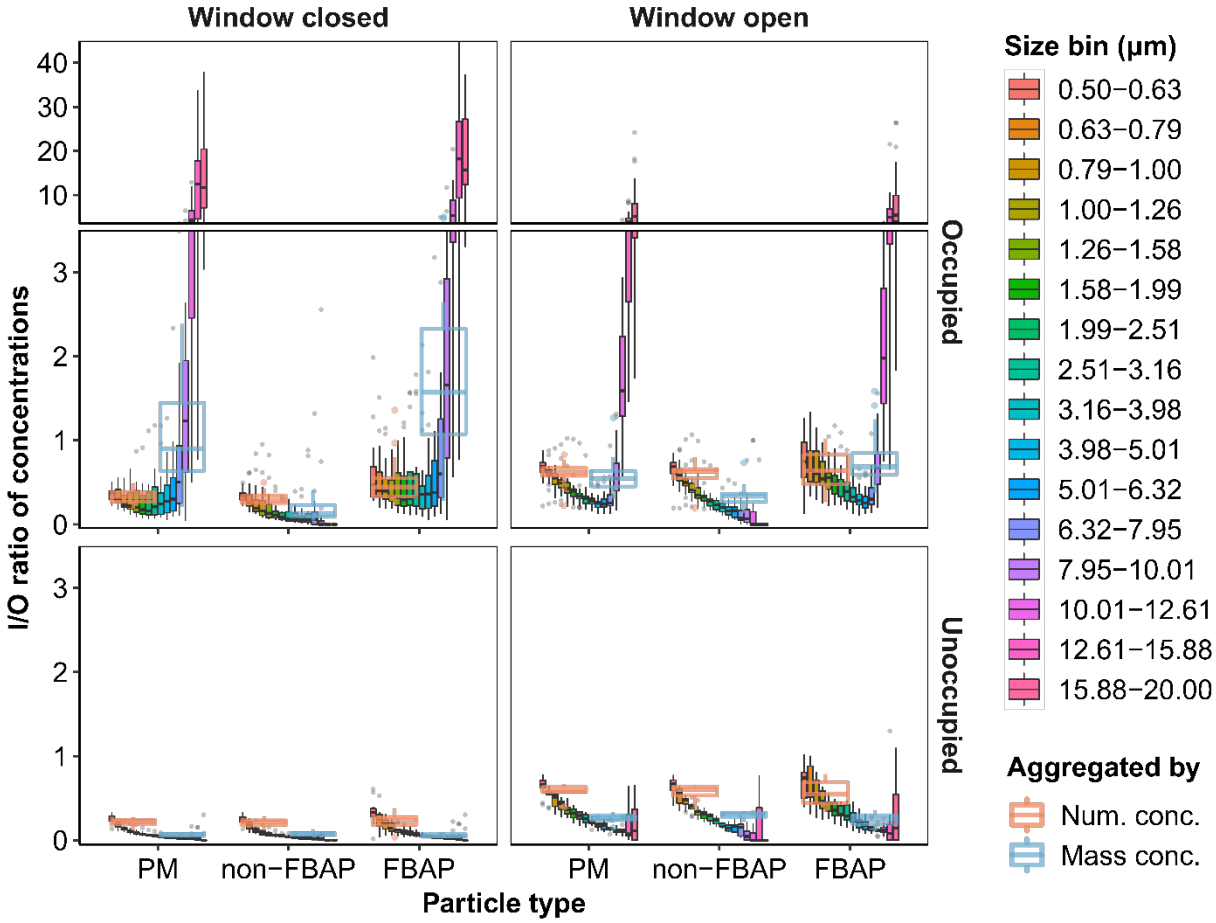

Figure 7. Effect of window and occupancy status on the I/O ratio of particle concentration. The color filled boxplots plot size-resolved results, and unfilled plots show the I/O ratios for aggregated size bins by number and mass concentrations.

For both non-FBAP and FBAP, the I/O ratios when the room was occupied were higher compared to when it was unoccupied for all size bins. The differences of FBAP between occupied and unoccupied periods were much larger than those of non-FBAP, especially for larger sized particles. This shows that the occupant was a source of both non-FBAP and FBAP, whereby FBAP had a larger bin size.

For this bedroom scenario, occupancy determined the indoor source strength of particles, while the window status affected the exchange degree between indoor and outdoor particles. When the room was unoccupied, the indoor particles originated from the outdoor

environment, opening the window increased the I/O ratio for both non-FBAP and FBAP at all size bins due to a higher infiltration rate, as shown in the bottom two subplots in Figure 7. However, when the occupant was in the room, opening the window increased the I/O ratio of non-FBAP for all size bins, but decreased the ratio of FBAP at 3.16-3.98 μm and bins with larger sizes. Dominated by FBAP in larger sizes, when PM was at and larger than 3.98-5.01 μm, its I/O ratio was lower when the window was open than it was closed. The effect of the window on I/O ratios indicated the source strength between the indoor and outdoor environment was different for different size bins and particle types. For non-FBAPs, even the occupant could be a source according to the previous paragraph, although its strength was weaker than outdoors for all size bins. For FBAPs, the indoor source was stronger than the outdoor one when the size was larger than 3.16 μm. Moreover, the mass concentration was dominated by the particles with larger sizes. When the window was closed, the lumped I/O ratio of PM and FBAP by the mass concentration was 1.6 and 2.3 times higher than it was open.

For other subtypes of FBAP, the mass aggregated I/O ratios of FL1 channel related types (i.e. A, AB, AC, and ABC) were lower when the window was open compared to when it was closed, but not for the other particles (detailed in Figure A6 in Appendix 1). We can deduce that, even the total amount of bioaerosols were mainly generated within the indoor environment, different kind of bioaerosols could have different sources.

4. DISCUSSION

4.1. Sources strength of aerosols in the bedroom

Under the assumption that infiltrated particles originate only from the outdoor environment, the mass balance method[40,41] was used to estimate the indoor source strength for all kinds of particles (detailed in the Appendix 1 S2). Without detailed recorded activities, each day of the experiment was separated into three periods with one-hour safety margins placed before and after unoccupied, awake, and asleep periods to calculate the indoor particle emission rates. The results of the number emission rate ($E_{N,activity}^{type}$ #/h) and the mass emission rate ($E_{M,activity}^{type}$, mg/h) were listed in Table 2.

Table 2. Number and mass emission rates for different particles by mean (SD).

	Unit	**Unoccupied**	**Awake**	**Sleep**
E_N^{PM}	# × 10⁶/h	1.0 (15.8)	94.5 (83.8)	37.4 (58.5)
$E_N^{non-FBAI}$	# × 10⁶/h	-3.9 (13.6)	48.6 (64.4)	18.7 (43.0)
E_N^{FBAP}	# × 10⁶/h	4.9 (6.1)	45.9 (34.2)	18.7 (18.4)
E_N^{A}	# × 10⁶/h	1.5 (1.4)	18.5 (30)	1.6 (1.5)
E_N^{B}	# × 10⁶/h	0.9 (2.6)	6.2 (8.0)	5.2 (7.5)
E_N^{C}	# × 10⁶/h	0.7 (1.6)	3.1 (2.3)	2.3 (2.4)
E_N^{AB}	# × 10⁶/h	0.4 (0.5)	3.5 (3.1)	0.7 (1.1)
E_N^{AC}	# × 10⁶/h	0.1 (0.2)	1.0 (1.1)	0.3 (0.3)
E_N^{BC}	# × 10⁶/h	0.9 (2.2)	3.5 (5.4)	4.0 (5.1)
E_N^{ABC}	# × 10⁶/h	0.4 (0.7)	10.2 (8.8)	4.6 (6.0)
E_M^{PM}	mg/h	0.02 (0.07)	5.09 (7.34)	2.88 (6.67)
$E_M^{non-FBAI}$	mg/h	-0.01 (0.02)	0.06 (0.11)	0.05 (0.16)
E_M^{FBAP}	mg/h	0.02 (0.06)	5.02 (7.28)	2.83 (5.91)
E_M^{A}	mg/h	0.00 (0.00)	0.06 (0.1)	0.01 (0.01)
E_M^{B}	mg/h	0.00 (0.01)	0.01 (0.02)	0.09 (0.27)
E_M^{C}	mg/h	0.00 (0.00)	0.01 (0.01)	0.01 (0.02)
E_M^{AB}	mg/h	0.00 (0.01)	0.05 (0.07)	0.17 (0.5)
E_M^{AC}	mg/h	0.00 (0.00)	0.01 (0.01)	0.02 (0.04)
E_M^{BC}	mg/h	0.00 (0.01)	0.02 (0.03)	0.01 (0.02)
E_M^{ABC}	mg/h	0.02 (0.06)	4.86 (7.27)	2.52 (5.06)

During the unoccupied periods, indoor emission rates of particles were around zero for all the size bins, which means the occupant or the occupant's activity were the major source of airborne particles in the bedroom. When the occupant was in the bedroom and awake, the mean indoor source strengths of PM were 94.5 # × 10⁶/h and 5.09 mg/h, and those of FBAPs

were 45.9 # × 10^6/h and 5.02 mg/h, by number and mass respectively, the resultant FBAP proportions of PM were 44% and 98%. While asleep, the emission rate was less than a one-half of when the occupant was awake. The FBAP proportion in the emitted particles was also higher. Comparing the FBAP proportions in PM in both environments, the proportions in emitted particles during occupied periods were much higher, which changed the PM composition between indoors and outdoors, as shown in Table 1. For subtypes of FBAPs, ABC had the highest indoor source strength regarding the mass emission rate during both the awake and sleep periods. For the emission rates by the number of particles, type A and B were the highest during the awake and sleep periods, respectively. Interestingly, type B and BC had higher emission rates by mass during the sleep periods than awake, but did not have those by number. This could be because the interaction of the occupant and the mattress and the human thermal plumes resuspended larger particles from the bed[17].

The size-resolved emission rates are shown in Appendix 1 (Figure A7, A8, and Table A4). The indoor emission rate in the first bin size (0.50-0.63 μm) was the highest by number, while the mass emission rate was dominated by the last two bins (i.e., 12.61-15.88 and 15.88-20.00 μm). Using the size resolved data, we can take a subset of the data to match the size range and compare the emission rate with previous studies. Using a previous version of WIBS with the measuring size range of 1 -10 μm, Zhou et al.[42] studied per person emission rates of FBAP when activity was to walk inside an environmental chamber. The emission rates ranged from 6.8 to 27.9 × 10^6 #/h according to different skin moister levels. After taking a subset of the data corresponding to the same size range, the mean (SD) count-based emission rate during the awake period in our study was 24.5 (20.0) × 10^6 #/h, which was comparable to Zhou et al.'s study. In another environmental chamber, Bhangar et al.[43] used a UV-APS to investigate the human emission rate of FBAP within a size range of 2.5-10 μm and reported 0.9 and 6.0 × 10^6 #/h per person under seated and walking conditions, respectively. To make results from WIBS and UV-APS comparable, we need to consider both size range and fluorescent channels. According to a side-by-side comparison between UV-APS and WIBS[44], the FL3 channel related particle type (i.e. C, AC, BC, and ABC) was selected for this comparison. After taking the subset, the mean (SD) of the count-based emission rate during awake period was 5.1 (4.4) × 10^6 #/h, which was comparing to the emission rate under the walking condition found in Bhangar et al.'s study. In summary, the bedroom FBAP source strength when the occupant was awake was comparable to those reported in previous studies under walking conditions in a chamber. When the occupant was awake, though the bedroom activities were mainly seated, some short-term bedroom activities could generate large amount of FBAPs, such as vacuum cleaning[45], arranging the bedsheets[46], and folding clothes[47], which made the averaged emission rate during the awake periods in the bedroom comparable to the emission rate under walking conditions in a controlled chamber.

4.2. Estimated contributions of indoor sources to indoor airborne particles

Using the size- and type-resolved emission rate under different activities (E_N^{ABC}, i denotes the i^{th} size bin in the total of n bins) and the outdoor concentration ($C_{\text{out},i}^{type}$), the indoor concentration (C_i^{type}) of each particle type can be estimated by Eq. (6).

$$C^{type} = \sum_{i=1}^{n}\left(\frac{a \cdot P}{a + k_i} C_{\text{out},i}^{type} + \frac{E_{activity,i}^{type}}{(a + k_i) \cdot V}\right) \quad (6)$$

The first term in the summation formula indicates the contribution of the outdoor sources and the second term shows that of indoor sources. Given two air change rates (a_{closed} =0.27 h^{-1}, and a_{open} =1.32 h^{-1}), the proportional contribution of indoor source to indoor airborne particles can be calculated by (7).

$$contr.in^{type} = \frac{\sum_{i=1}^{n} E_{activity,i}^{type}}{\sum_{i=1}^{n} E_{activity,i}^{type} + \sum_{i=1}^{n} V \cdot a \cdot P \cdot C_{\text{out},i}^{type}} \times 100\% \quad (7)$$

Using the median outdoor concentration and the emission rates under different activities, the proportional contribution of the indoor source both when the window was closed and open was calculated and listed in Table 3.

Table 3. Contributions of the indoor source to indoor particles in proportions (%)

	By number				By mass			
	Closed		Open		Closed		Open	
	Awake	Sleep	Awake	Sleep	Awake	Sleep	Awake	Sleep
PM	48.0	28.2	16.3	7.5	94.2	90.4	80.0	70.1
non-FBAP	40.3	22.0	12.1	5.3	47.2	33.6	15.7	10.5
FBAP	71.0	51.9	34.4	18.4	97.6	95.7	90.1	83.3
A	89.0	42.8	63.1	13.4	93.5	55.7	74.8	20.7
B	49.6	47.3	16.8	15.3	61.5	83.5	25.1	55.5
C	64.4	58.6	27.2	22.3	70.8	68.3	32.8	31.1
AB	74.6	42.1	39.6	13.2	90.1	94.6	65.2	79.6
AC	90.3	69.6	66.5	32.8	93.5	93.1	74.3	74.5
BC	63.0	68.3	26.2	30.4	72.3	67.5	34.8	29.0
ABC	87.3	76.4	60.0	40.6	99.0	98.1	95.4	91.4

From Table 3, the contribution of indoor source to indoor particles decreased when we opened the window. The number concentration of indoor FBAP was dominated by the indoor source when the window was closed (i.e. more than 50%), while the mass concentration was always dominated by the indoor source no matter the window condition. In contrast, indoor non-FBAP was always dominated by outdoor sources. Most of subtypes of FBAPs (except type B by number) were dominated by indoor sources by a various degree in proportions.

4.3. Relationship between the indoor bioaerosol exposure and window conditions

As shown in Eq. (6), given the condition of the window (open or closed) and the activity (sleep or awake), the indoor and outdoor concentrations form a linear relationship. We assume that the proportioned size and type distribution are relatively stable in the outdoor environment, denoted as $size.prop_i^{PM}$ and $type.prop_i^{type}$, respectively, which can be found in Results 3.1 and 3.2 with the uncertainty (IQR) less than 10% for FBAPs. We can obtain the outdoor concentration of each particle type ($C_{\text{out},i}^{type}$) by outdoor PM levels (C_{out}^{PM}) using Eq. (8). By substituting Eq. (8) into Eq. (6), we can estimate the indoor concentration of each particle

type (C^{type}) under each activity by using outdoor PM concentrations (C^{PM}_{out}), as shown in Appendix 1 (Figure A9).

$$C^{type}_{out,i} = C^{PM}_{out} \cdot size.prop^{PM}_{i} \cdot type.prop^{type}_{i} \quad (8)$$

From Figure A9, when C^{PM}_{out} is lower than 19.1 μg/m³ and when the occupant is awake (or, when C^{PM}_{out} < 9.9 μg/m³ and when the occupant is sleeping), we should open the window to lower indoor FBAP levels. The periods when C^{PM}_{out} was lower than 19.1 and 9.9 μg/m³ account for 21.1% and 74.8% of the total experiment period, respectively. Hence, for most of the time in that month in Singapore, opening the window can have a lower level of indoor bioaerosol exposure when the occupant was awake at home, while it was better to close the window when sleep regarding the level of bioaerosol exposure.

Furthermore, with higher uncertainty, we can generalize the results by using widely reported air quality station data as an indicator to decide whether we should open the window. In Singapore, 24-hourly averaged outdoor mass concentrations of $PM_{<2.5}$ and $PM_{<10}$ (i.e., PM with a diameter smaller than 2.5 and 10 μm, respectively) are reported by the National Environment Agency and updated hourly. The overlapped size range between the outdoor concentration (C^{PM}_{out}) in this study and the station-reported PM concentrations is from 2.5 to 10 μm, and the mass concentrations were noted as $C^{PM}_{out,\,2.5\text{-}10}$ and $C^{PM}_{station,2.5-10}$ in μg/m³, respectively. The data from the central station (1°21'26.5"N 103°49'12.0"E) was selected because its location was the nearest one to the sampling site (1°18'20.9"N 103°45'43.5"E). The relationship between $C^{PM}_{out,\,2.5\text{-}10}$ and $C^{PM}_{station,2.5-10}$ are written in Eq. (9), and the coefficient ($coef$) was equal to 0.73 (R^2 = 0.96), which from derived from a linear regression, as shown in Appendix 1 (Figure A10).

Using the proportion of outdoor particles within the size range of 2.5-10 μm in total ($size.prop^{PM}_{2.5-10}$ = 55.6% from the proportioned size distribution of PM in Section 3.1), we can get the outdoor concentration of PM (C^{PM}_{out}) by Eq. (10). By substituting Eq.(8) and (10) back into Eq. (6), we obtain the relationship between the indoor concentration of each particle type (C^{type}) and $C^{PM}_{station,2.5-10}$, as shown in Eq. (11). Under different window and indoor activity conditions, the relationship between indoor FBAP concentration (C^{FBAP}) and $C^{PM}_{station,2.5-10}$ was plotted in Figure 8.

$$C^{PM}_{out,2.5-10} = coef \cdot C^{PM}_{station,2.5-10} = 0.73 \cdot C^{PM}_{station,2.5-10} \quad (9)$$

$$C_{\text{Out}}^{PM} = \frac{C_{\text{out},2.5-10}^{PM}}{size.prop_{2.5-10}^{PM}} = \frac{C_{\text{out},2.5-10}^{PM}}{55.6\%} = \frac{0.73 \cdot C_{station,2.5-10}^{PM}}{55.6\%} \quad (10)$$

$$C^{type} = \sum_{i=1}^{n} \left(\frac{P \cdot ACH}{ACH + k_i} \frac{C_{station,2.5-10}^{PM} \cdot coef}{size.prop_{2.5-10}^{PM}} \cdot size.prop_i^{PM} \cdot type.prop_i^{type} + \frac{E_i^{type}}{(ACH + k_i) \cdot V} \right) \quad (11)$$

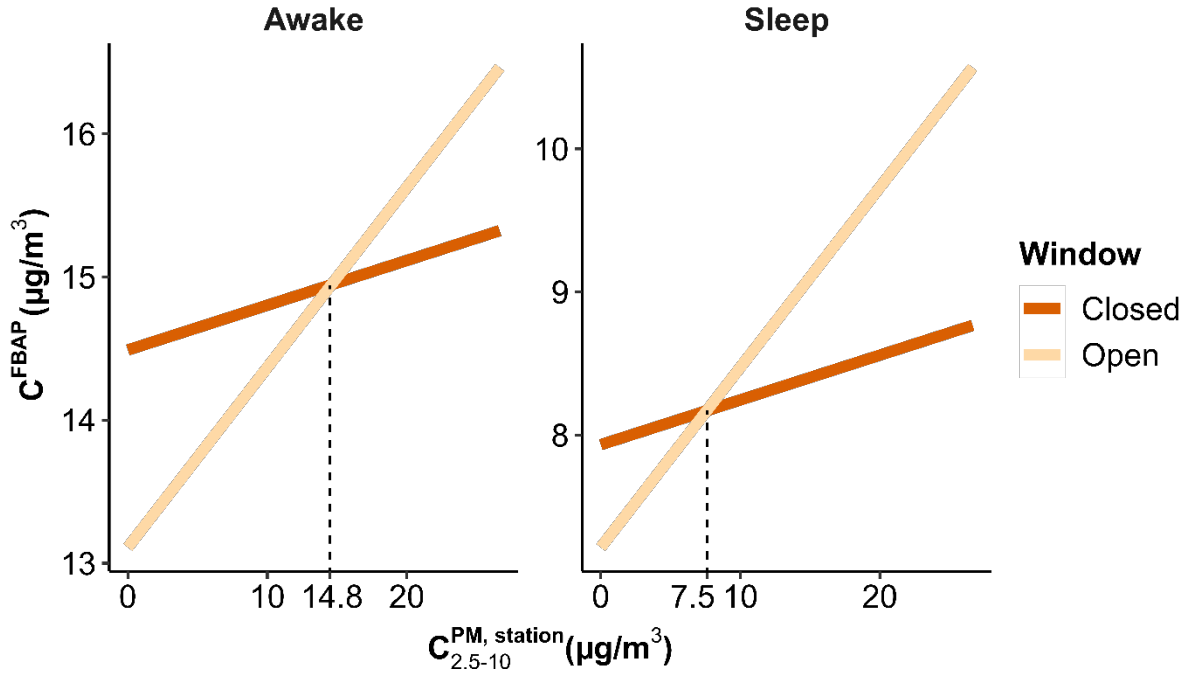

Figure 8. Estimation of indoor FBAP mass concentration based on the difference between station-reported $PM_{<2.5}$ and $PM_{<10}$ concentrations

In Figure 8, two lines show the estimated relationship between $C_{station,2.5-10}^{PM}$ and C^{FBAP} when the window was open or closed, respectively. When the window is open, the slopes are larger than when it is closed, while the intercepts were smaller. Before the intersection of two lines, the indoor concentration is lower when the window is open than it is closed. For FBAPs, the $C_{station,2.5-10}^{PM}$ on the intersection point is noted as the upper bound for opening the window (UB_{open}^{FBAP}). The UB_{open}^{FBAP} during the awake and sleep periods were 14.8 µg/m³ and 7.5 µg/m³, respectively, which were higher than the value during 20.3% and 89.6% of reported $C_{station,2.5-10}^{PM}$ throughout the whole year of 2019 in Singapore. For other types of particle, the UB_{open}^{type} was calculated according to its indoor source strengths, size and type proportions in PM, and listed in Table 4. Though biological implications of the reported subtypes of the

FBAP is currently unclear, these type-resolved indicators could potentially help us to develop a more targeted strategy to mitigate certain classes of bioaerosols.

Table 4. The estimated UB_{open}^{type} for different particles (μg/m³)

	PM	non-FBAP	FBAP	A	B	C	AB	AC	BC	ABC
Awake	7.1	1.3	14.8	13.2	1.8	2.3	5.6	9.1	1.9	27.7
Sleep	3.9	0.5	7.5	1.1	2.9	1.8	5.6	5.5	1.8	14.9

4.4. Limitations and future directions

Besides the uncertainty from the fluorescent signals mentioned above, we will discuss more limitations of this study.

First, these findings from this paper are limited by the single case study. Despite this room has certain representativeness of common living conditions in Singapore, we still need more cases to verify the results. For further studies, using the same methodology developed from this study, we plan to test more cases of different building types and different ventilation systems.

Second, with focused on size-resolved relationships between biological and non-biological, and indoor and outdoor aerosols, we haven't considered the temporal variation of aerosols in this study. Time-resolved data from WIBS has the potential to identify the source of aerosols. This study already considered indoor sources of bioaerosols in relatively long periods, and we will further break it down and related them to different activities in further studies.

Lastly, along with the particle size, WIBS also provides the asymmetry for each particle. We haven't put this parameter in this study. The "shape" information is very important for species identification, which we will take this parameter into consideration for further species related analyses.

5. CONCLUSIONS

Major findings throughout the one-month measurement of indoor and outdoor bioaerosol sampling using two units of WIBS in a bedroom are:

1. For both indoor and outdoor environments from this case study in Singapore, the median (IQR) number concentrations of PM were 3.7 (2.7) and 7.8 (3.1) #/cm³, and FBAPs were 0.7 (0.5) and 1.4 (0.7) #/cm³, which resulted in a higher FBAP proportion in PM indoors compared to the outdoors (19% *vs.* 17%).
2. With the increase of particle size, concentrations of both FBAP and non-FBAP particles decreased but in different degrees. After 2 μm and 3.5 μm for the indoor and

outdoor environments, respectively, the amount of FBAPs became larger than that of non-FBAPs.

3. For the particles within the first bin size (0.50-0.63 μm), around 89% and 91% particles were non-FBAPs for indoor and outdoor, respectively. The proportion of FBAP in PM for each size bin in indoors was always higher than those in outdoors. Especially particles within 1.58 – 10.00 μm, the fluorescent proportions indoors were 10 – 17% higher than those in outdoors.
4. The occupant dominated the indoor source of both FBAPs and non-FBAPs. When awake or asleep, count- and mass-based emission rates were 45.9 (34.2) and 18.7 (18.4) × 10^6 #/h and 5.02 (7.28) and 2.83 (5.91) mg/h by mean (SD), respectively.
5. Based on the I/O ratios of FBAP under different conditions, indoor FBAPs larger than 3.16 μm were dominated by indoor sources, while indoor non-FBAPs mainly originated from the outdoor environment. Opening the window was an effective way to mitigate mass-based PM and FBAP exposures.

REFERENCES

1. Brunekreef B, Holgate ST. Air pollution and health. *The Lancet*. 2002;360(9341): 1233-1242. doi:10.1016/S0140-6736(02)11274-8

2. Fisk WJ. Health benefits of particle filtration. *Indoor Air*. 2013;23(5):357-368. doi: 10.1111/ina.12036

3. Lippmann M. Health effects of airborne particulate matter. *N Engl J Med*. 2007;357(23): 2395-2397. doi:10.1056/NEJMe0706955

4. Zhou M, Wang H, Zeng X, et al. Mortality, morbidity, and risk factors in China and its provinces, 1990–2017: a systematic analysis for the Global Burden of Disease Study 2017. *The Lancet*. 2019;394(10204):1145-1158. doi:10.1016/S0140-6736(19)30427-1

5. Guarnieri M, Balmes JR. Outdoor air pollution and asthma. *The Lancet*. 2014;383(9928): 1581-1592. doi:10.1016/S0140-6736(14)60617-6

6. Kim K-H, Kabir E, Kabir S. A review on the human health impact of airborne particulate matter. *Environ Int*. 2015;74:136-143. doi:10.1016/j.envint.2014.10.005

7. Després VivianeR, Huffman JA, Burrows SM, et al. Primary biological aerosol particles in the atmosphere: a review. *Tellus B Chem Phys Meteorol*. 2012;64(1):15598. doi: 10.3402/tellusb.v64i0.15598

8. Tesson SVM, Skjøth CA, Šantl-Temkiv T, Löndahl J. Airborne microalgae: Insights, opportunities, and challenges. *Appl Env Microbiol*. 2016;82(7):1978-1991. doi:10.1128/AEM.03333-15

9. Jaenicke R. Abundance of Cellular Material and Proteins in the Atmosphere. *Science*. 2005;308(5718):73-73. doi:10.1126/science.1106335

10. Douwes J, Thorne P, Pearce N, Heederik D. Bioaerosol health effects and exposure assessment: progress and prospects. *Ann Occup Hyg*. 2003;47(3):187–200.

11. Walser SM, Gerstner DG, Brenner B, et al. Evaluation of exposure–response relationships for health effects of microbial bioaerosols – A systematic review. *Int J Hyg Environ Health*. 2015;218(7):577-589. doi:10.1016/j.ijheh.2015.07.004

12. Coleman KK, Nguyen TT, Yadana S, Hansen-Estruch C, Lindsley WG, Gray GC. Bioaerosol sampling for respiratory viruses in Singapore's Mass Rapid Transit network. *Sci Rep*. 2018;8(1):17476.

13. Ooi PL, Goh KT, Phoon MH, Foo SC, Yap HM. Epidemiology of sick building syndrome and its associated risk factors in Singapore. *Occup Environ Med*. 1998;55(3):188-193. doi:10.1136/oem.55.3.188

14. Zuraimi MS, Tham KW. Indoor air quality and its determinants in tropical child care centers. *Atmos Environ*. 2008;42(9):2225-2239. doi:10.1016/j.atmosenv.2007.11.041

15. Heald CL, Spracklen DV. Atmospheric budget of primary biological aerosol particles from fungal spores. *Geophys Res Lett*. 2009;36(9). doi:10.1029/2009GL037493

16. Lan L, Tsuzuki K, Liu YF, Lian ZW. Thermal environment and sleep quality: A review. *Energy Build*. 2017;149:101-113. doi:10.1016/j.enbuild.2017.05.043

17. Boor BE, Spilak MP, Laverge J, Novoselac A, Xu Y. Human exposure to indoor air pollutants in sleep microenvironments: A literature review. *Build Environ*. 2017;125:528-555. doi:10.1016/j.buildenv.2017.08.050

18. Allen JG, Cedeno-Laurent JG, Jones E, et al. *Homes for Health: 36 Expert Tips to Make Your Home a Healthier Home*. Harvard T.H. Chan School of Public Health; 2019:28. www.ForHealth.org.

19. Mishra AK, van Ruitenbeek AM, Loomans MGLC, Kort HSM. Window/door opening-mediated bedroom ventilation and its impact on sleep quality of healthy, young adults. *Indoor Air*. 2018;28(2):339-351. doi:10.1111/ina.12435

20. Zanobetti A, Redline S, Schwartz J, et al. Associations of PM10 with sleep and sleep-disordered breathing in adults from seven US urban areas. *Am J Respir Crit Care Med*. 2010;182(6):819-825. doi:10.1164/rccm.200912-1797OC

21. Strøm−Tejsen P, Zukowska D, Wargocki P, Wyon DP. The effects of bedroom air quality on sleep and next-day performance. *Indoor Air*. 2016;26(5):679-686. doi:10.1111/ina.12254

22. Housing & Development Board. *Annual Reports - Housing & Development Board (HDB)*.; 2018. https://www.hdb.gov.sg/cs/infoweb/about-us/news-and-publications/annual-reports. Accessed June 9, 2019.

23. Griffiths WD, DeCosemo GAL. The assessment of bioaerosols: A critical review. *J Aerosol Sci*. 1994;25(8):1425-1458. doi:10.1016/0021-8502(94)90218-6

24. Blais-Lecours P, Perrott P, Duchaine C. Non-culturable bioaerosols in indoor settings: Impact on health and molecular approaches for detection. *Atmos Environ*. 2015;110:45-53. doi:10.1016/j.atmosenv.2015.03.039

25. Nazaroff WW. Indoor bioaerosol dynamics. *Indoor Air*. 2016;26(1):61-78. doi:10.1111/ina.12174

26. Pöhlker C, Huffman JA, Pöschl U. Autofluorescence of atmospheric bioaerosols – fluorescent biomolecules and potential interferences. *Atmospheric Meas Tech*. 2012;5(1):37-71. doi:10.5194/amt-5-37-2012

27. Fennelly M, Sewell G, Prentice M, et al. The use of real-time fluorescence instrumentation to monitor ambient primary biological aerosol particles (PBAP). *Atmosphere*. 2017;9(1):1. doi:10.3390/atmos9010001

28. Gabey AM, Gallagher MW, Whitehead J, Dorsey JR, Kaye PH, Stanley WR. Measurements and comparison of primary biological aerosol above and below a tropical forest canopy using a dual channel fluorescence spectrometer. *Atmospheric Chem Phys*. 2010;10(10):4453-4466. doi:10.5194/acp-10-4453-2010

29. Perring AE, Schwarz JP, Baumgardner D, et al. Airborne observations of regional variation in fluorescent aerosol across the United States. *J Geophys Res Atmospheres*. 2015;120(3):1153-1170. doi:10.1002/2014JD022495

30. Hernandez M, Perring AE, McCabe K, Kok G, Granger G, Baumgardner D. Chamber catalogues of optical and fluorescent signatures distinguish bioaerosol classes. *Atmospheric Meas Tech*. 2016;9(7):3283-3292. doi:10.5194/amt-9-3283-2016

31. Savage NJ, Krentz CE, Könemann T, et al. Systematic characterization and fluorescence threshold strategies for the wideband integrated bioaerosol sensor (WIBS) using size-resolved biological and interfering particles. *Atmospheric Meas Tech*. 2017;10(11): 4279-4302. doi:10.5194/amt-10-4279-2017

32. Pitz M, Schmid O, Heinrich J, et al. Seasonal and Diurnal Variation of PM2.5 Apparent Particle Density in Urban Air in Augsburg, Germany. *Environ Sci Technol*. 2008;42(14): 5087-5093. doi:10.1021/es7028735

33. Hu M, Peng J, Sun K, et al. Estimation of size-resolved ambient particle density based on the measurement of aerosol number, mass, and chemical size distributions in the winter in Beijing. *Environ Sci Technol*. 2012;46(18):9941-9947. doi:10.1021/es204073t

34. Fischer B, Pau G, Smith M, Morgan M, Twisk D van. *Rhdf5: R Interface to HDF5*. Bioconductor version: Release (3.9); 2019. doi:10.18129/B9.bioc.rhdf5

35. Wickham H. *Tidyverse: Easily Install and Load the "Tidyverse."*; 2017. https://CRAN.R-project.org/package=tidyverse. Accessed October 12, 2019.

36. Dowle M, Srinivasan A, Gorecki J, et al. *Data.Table: Extension of "Data.Frame."*; 2019. https://CRAN.R-project.org/package=data.table. Accessed October 12, 2019.

37. Wickham H, Chang W, Henry L, et al. *Ggplot2: Create Elegant Data Visualisations Using the Grammar of Graphics*.; 2019. https://CRAN.R-project.org/package=ggplot2. Accessed October 12, 2019.

38. Pedersen TL. *Thomasp85/Patchwork*.; 2019. https://github.com/thomasp85/patchwork. Accessed October 12, 2019.

39. Calvo AI, Baumgardner D, Castro A, et al. Daily behavior of urban fluorescing aerosol particles in northwest Spain. *Atmos Environ*. 2018;184:262-277. doi:10.1016/j.atmosenv.2018.04.027

40. Priyamvada H, Priyanka C, Singh RK, Akila M, Ravikrishna R, Gunthe SS. Assessment of PM and bioaerosols at diverse indoor environments in a southern tropical Indian region. *Build Environ*. 2018;137:215-225. doi:10.1016/j.buildenv.2018.04.016

41. Qian J, Hospodsky D, Yamamoto N, Nazaroff WW, Peccia J. Size-resolved emission rates of airborne bacteria and fungi in an occupied classroom. *Indoor Air*. 2012;22(4): 339-351. doi:10.1111/j.1600-0668.2012.00769.x

42. Zhou J, Fang W, Cao Q, Yang L, Chang VW-C, Nazaroff WW. Influence of moisturizer and relative humidity on human emissions of fluorescent biological aerosol particles. *Indoor Air*. 2017;27(3):587-598. doi:10.1111/ina.12349

43. Bhangar S, Adams RI, Pasut W, et al. Chamber bioaerosol study: human emissions of size−resolved fluorescent biological aerosol particles. *Indoor Air*. 2016;26(2):193-206. doi:10.1111/ina.12195

44. Healy DA, Huffman JA, O'Connor DJ, Pöhlker C, Pöschl U, Sodeau JR. Ambient measurements of biological aerosol particles near Killarney, Ireland: a comparison between real-time fluorescence and microscopy techniques. *Atmospheric Chem Phys*. 2014;14(15):8055-8069. doi:https://doi.org/10.5194/acp-14-8055-2014

45. Knibbs LD, He C, Duchaine C, Morawska L. Vacuum cleaner emissions as a source of indoor exposure to airborne particles and bacteria. *Environ Sci Technol*. 2012;46(1): 534-542. doi:10.1021/es202946w

46. Yen Y-C, Yang C-Y, Mena KD, Cheng Y-T, Yuan C-S, Chen P-S. Jumping on the bed and associated increases of PM10, PM2.5, PM1, airborne endotoxin, bacteria, and fungi concentrations. *Environ Pollut*. 2019;245:799-809. doi:10.1016/j.envpol.2018.11.053

47. Tian Y, Liu Y, Misztal PK, et al. Fluorescent biological aerosol particles: Concentrations, emissions, and exposures in a northern California residence. *Indoor Air*. 2018;28(4): 559-571. doi:10.1111/ina.12461